Investigation of the Gas-Phase Amino Acid Alanine by Synchrotron Radiation Photoelectron Spectroscopy

Ivan Powis,*,† Emma E. Rennie,‡,§,|| Uwe Hergenhahn,‡,§ Oliver Kugeler,‡,§ and Reagan Bussy-Socrate†

School of Chemistry, University of Nottingham, Nottingham NG7 2RD, U.K., Fritz-Haber Institut der Max Planck Gesellschaft, Faradayweg 4-6, D-14195 Berlin, Germany, and Max-Planck-Institute for Plasma Physics, Boltzmannstr. 2, D-85748 Garching, Germany

Received: July 29, 2002; In Final Form: October 30, 2002

Valence and C1s core level photoelectron spectra of gaseous alanine have been recorded with synchrotron radiation. Using ab initio Green's Function calculations of the vertical outer valence ionization energies and CMS-Xα calculations of the orbital ionization cross-sections, it is possible to account well for the features of both the new $h\nu = 92$ eV valence photoelectron spectrum and also its differences with an earlier $h\nu = 21.2$ eV spectrum. Good agreement may be achieved by considering just the contribution of a single molecular conformation. This agrees with previous experimental findings, but conflicts with calculations which suggest that a range of molecular conformations would coexist in an equilibrium sample. A study of the valence photoelectron spectrum of the amino acid threonine complements that of alanine, but unlike the latter is limited by the effects of thermal decomposition of the sample. The C1s core level spectrum of alanine is reported and its peaks are assigned to ionization of the three C atoms in the molecule. A fourth minor peak that is observed is tentatively assigned to a peptide $\underline{\mathbf{C}}ONH_2$ linkage which may be formed between alanine monomers.

1. Introduction

While the simplest amino acid is glycine (NH_2CH_2COOH), the next member of the series, alanine ($CH_3CH(NH_2)COOH$), is the first *chiral* amino acid having distinct enantiomeric structures; both thus provide significant prototypes for developing our understanding of this important class of molecule.

The range of inter- and intramolecular interactions that can be envisaged for these species lends a rich variety and complexity to the possible geometric and electronic structural forms that they may adopt. In the solid phase, the monomer species exist in zwitterionic form (i.e., $>C(NH_3^+)COO^-$ with a proton transferred from the carboxylic acid to the amino group),[1] while in solution cationic, anionic, and zwitterionic structures are all found depending on the pH. Adsorption on metal surfaces may lead to de-protonation of the carboxylic acid group with the bonding to the metal involving both carboxylic and amino functional groups.[2,3] Finally, the potential for polymerization via peptide linkages is of biological significance.

Although it might then appear that the study of isolated molecules in the gas phase would be more straightforward, such investigations have been very limited. Experimentally, the low volatility of the amino acids provides a significant challenge. Even so, the limited data available to date raises important issues yet to be fully understood. Calculations suggest that while free, isolated alanine[4−7] exists in molecular form, it may adopt a number of different conformations. The predicted relative stability of these is dependent upon the subtle interplay of a variety of intramolecular hydrogen bonding and electron correlation, and so precise predictions prove to vary somewhat with the method of computation. Nevertheless, of the thirteen conformers identified in these studies, the lowest lying are evidently so close in energy that, at the elevated temperatures required for experiments, one could expect several to coexist with comparable populations.

Surprisingly then, the first structural determination by gas-phase electron diffraction[8] found evidence for the existence of only a single conformer, **1** (see Figure 1). A later rotational spectroscopy experiment[9] identified a second alanine conformer structure, **3**, though the earlier conformer **1** remained in an estimated 8-fold excess. A third expected structure, **2**, was not detected, nor were a number of other conformers (**4**,**5**) expected to lie approximately 400 cm^{-1} higher in energy. Subsequently a second electron diffraction study[10] and a re-appraised data analysis guided by the rotational spectroscopy result[9] and calculations[7] has lent support to this finding of the coexistence of conformers **1**,**3** in an 8:1 ratio with, essentially, an absence of all other predicted conformers.

Very little other gas-phase data on alanine has been obtained other than He I photoelectron spectra.[11−13] As usual, these may be interpreted to yield information on the electronic structure of the molecule. It has also been recently pointed out[14] that these low-resolution He I photoelectron spectra (PES) appear to result predominantly from the same single conformer, **1**, as discussed above.

Although it may be possible to rationalize the nonobservance of some of the predicted conformer pairs by considering the possibility of their ready interconversion by large amplitude vibration,[5] certain discrepancies remain. A major difficulty in assessing the significance of the rotational spectroscopy result

* Corresponding author. Tel: +44 115 951 3467. Fax: +44 115 951 3562. E-mail: Ivan.Powis@Nottingham.ac.uk.
† University of Nottingham.
‡ Fritz-Haber Institut der Max Planck Gesellschaft.
§ Max-Planck-Institute for Plasma Physics.
|| Present address: Dept. of Chemistry, University of Ottawa, 10 Marie-Curie, Ottawa, Ontario K1N 6N5, Canada.

10.1021/jp0266345 CCC: $25.00
Published on Web 12/11/2002

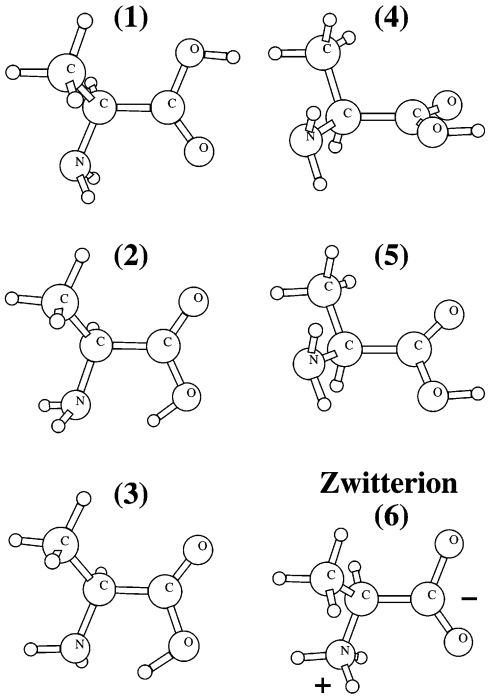

Figure 1. Conformations of L-alanine. The numbering of the low-energy conformers (**1**−**5**) corresponds to that used in refs 5,6,14, and to **I, IIB**, **IIA**, **IIIA**, **IIIB**, respectively, of ref 7. Structure **6** is a postulated zwitterionic form discussed in the text.

is the use of a free jet expansion in those experiments,[5,9] meaning that a true thermal equilibrium was almost certainly not obtained. However, one may assume that this objection does not apply to the electron diffraction experiments, nor to the photoelectron measurements. But then at the ∼500 K temperature of all these experiments, the reported population ratio of at least 8:1 is many times greater than the expected Boltzmann population ratio predicted from calculated energies of **1** and **3**, seeming to suggest a much bigger energy separation than is calculated.

Developing a better understanding of the structure of free gas-phase alanine, the existence and stability of its predicted conformers, and the intramolecular forces which govern this is an important prelude to understanding the structure and intermolecular interactions which are so important in the condensed phases of this and other amino acids. There is also a real intrinsic importance to developing a full understanding of the gas-phase structure(s) since it is required to guide and interpret searches for such a significant bio-organic species in the interstellar medium.

Our objective in this paper is then to develop, extend, and improve the analysis of gas-phase alanine photoelectron spectra. The use of synchrotron radiation allows the valence ionization region to be recorded with the range of ionization energies extending to the inner valence region and with a better sensitivity than hitherto achieved across the range. The experimental data are complemented by theoretical calculations of the vertical ionization energies and photon energy-dependent cross-sections for the low-lying conformers in Figure 1. We also present briefly some complementary PES data for another amino acid, threonine. In addition to the valence PES, we include measurements of the C1s core-level X-ray photoelectron spectrum (XPS) of alanine. Although the XPS of solid alanine has been measured previously[1] and used to infer its zwitterionic form, we are not aware of any previous study of the gas-phase XPS.

2. Experimental Details and Data Analysis

Spectra were recorded on the UE56/2-PGM[15] undulator beamline at the BESSY II synchrotron radiation source in Berlin with a Scienta SES-200 hemispherical electron spectrometer[16] mounted in a large spherical chamber. The beamline provides both linearly and circularly polarized light in an energy range extending from about 60 eV to 1400 eV. All of the spectra in this work were measured with circularly polarized light using a 400 l/mm grating. The hemispherical electron analyzer[16] was mounted outside of the dipole plane, under a forward scattering angle of 54.7° with respect to the beam direction. Under these conditions the electron acceptance of the analyzer is set at the "magic" angle so that measurements should be insensitive to the photoelectron asymmetry parameter, β.

Commercial samples of (*S*)-(+)-alanine (L) and (2*S*)(3*R*)-(−)-threonine (L) (Aldrich) were used without further purification. These very low vapor pressure molecules are solid at room temperature and so were sublimed in an oven immediately before entering a gas cell inside the main vacuum chamber. This cell has open sidearms for the synchrotron radiation beam to pass through and a further aperture for the generated photoelectrons to enter the Scienta input lens stack. The cell is also equipped with a photoelectron dump to prevent backscattered electrons from entering the analyzer. The temperature of the oven was measured with a thermoelement.

The (*S*)-(+)-alanine (L) valence spectrum was recorded with an incident photon energy of 92 eV. The spectrum was obtained with a beamline exit slit setting of ∼60 μm, an electron analyzer slit width of 0.2 mm and a pass energy of 40 eV, corresponding to an overall estimated resolution of 90 meV. To keep a constant pressure of approximately 1×10^{-6} mbar in the main chamber, the temperature of the oven was set to 268 °C. We estimate the pressure in the photoionization cell to be one or two orders of magnitude higher than the indicated chamber pressure. The spectra have been corrected for the $1/E_k^{1/2}$ instrument transmission function[16,17] (where E_k is the electron kinetic energy).

C1s core level spectra of alanine were recorded at photon energies of 309 and 301 eV. While the 40 eV electron analyzer pass energy of 40 eV was retained, the beamline exit slit was opened to 120 μm and the electron analyzer slit set to 0.5 mm, yielding an electron energy resolution of ∼200 meV. In the spectrum to be shown here, successive scans recorded with left and right circularly polarized light are summed together to cancel any residual intensity variations which might arise with an enantiomerically pure molecular sample. This precaution was not taken with the valence spectra, as such effects are not expected to be significant at the much higher electron energies (>50 eV) encountered in these latter studies.[14]

The (2*S*)(3*R*)-(−)-threonine (L) valence spectra were recorded with an incident photon energy of 92 eV. The oven temperature was varied between 147 °C up to ∼220 °C (corresponding indicated chamber pressures were $\leq 5 \times 10^{-6}$ mbar) and spectra were recorded at different temperatures in this range. Low-resolution spectra monitoring the temperature dependence were obtained with a beamline exit slit setting of ∼180 μm, an electron analyzer slit width of 1.0 mm, and a pass energy of 40 eV, corresponding to an overall estimated resolution of 300 meV. Higher-resolution spectra (∼211 °C) shown here were recorded with settings similar to those for alanine, described above.

3. Computational Details

Structural parameters for the various molecular conformations considered in this paper were determined from density functional

TABLE 1: Energies of Optimized Alanine Conformers

	B3LYP/6-31G**		MP2/6-311++G**	
conformer	absolute (a.u.)	relative (cm^{-1})	absolute (a.u.)	relative (cm^{-1})
1	−323.757175	0	−323.103014	0
2	−323.757713	−118	−323.102256	166
3	−323.756965	46	−323.102783	51
4	−323.754851	510	−323.101490	334
5	−323.754761	530	(−323.100969)[a]	(449)[a]

[a] Values reported in ref 7.

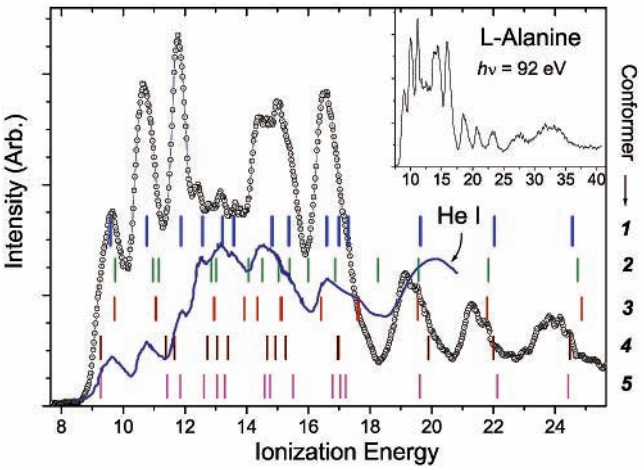

Figure 2. Valence photoelectron spectrum of L-alanine, $h\nu = 92$ eV. Calculated ROVGF/cc-pVDZ//B3LYP/6-31G** vertical ionization energies for each conformer **1**−**5** are marked on the plot. A He I spectrum (derived from ref 12) is included for comparison. The inset shows a full-range scan including the complete inner-valence region.

theory full geometry optimizations undertaken to locate the local minima. A B3LYP functional[18,19] and 6-31G** basis set were used for this purpose, as implemented in the Gaussian 98 package.[20] For the main conformers of alanine alternative optimized geometries were calculated at the full MP2 level using an augmented 6-311++G** basis set.

Theoretical estimates of the vertical ionization energies for each geometry were calculated using an outer-valence Green's function (OVGF) method[21,22] and a cc-pVDZ basis, again using the Gaussian 98 package.[20]

Photoionization cross-sections were likewise obtained for the alanine conformers by a continuum multiple scattering treatment, utilizing an Xα local-exchange potential, (CMS-Xα).[23,24] Self-consistent overlapping sphere model Xα potentials were obtained for each B3LYP/6-31G** molecular geometry. These neutral molecule ground-state potentials were then adapted to have the correct long-range Coulombic form appropriate to the ionic state and were subsequently used to calculate the ground-state continuum matrix elements for each assumed conformation. Further details of the method and procedures adopted may be found in ref 25.

4. Results and Discussion

4.1. Valence Photoelectron Spectra. *4.1.1. Alanine Valence Photoelectron Spectrum.* The photoelectron spectrum of alanine, recorded with a photon energy $h\nu = 92$ eV, is displayed in Figure 2. While the inset shows an overview of the complete scan, the main figure shows a smoothed spectrum of the outer valence region in greater detail. Also included is a representation of the He I spectrum.[12] It can be seen there is a good correspondence between the peak positions evident in the two spectra. Equally, it can be seen that the relative intensity of the first three visible structures is enhanced, that of the second three suppressed in the $h\nu = 92$ eV spectrum compared to the He I ($h\nu = 21.2$ eV) spectrum. The broad bands seen in the highly correlated inner valence region above 25 eV fall outside the scope of the independent particle ionization treatments adopted here, and will not be further discussed here.

The B3LYP/6-31G** and MP2/6-311++G** energies obtained from our calculations for the various alanine conformers **1**−**5** are summarized in Table 1. The latter results essentially replicate those previously reported by Csaszar[7] at the same level, with the exception that we were unable to locate a stable minimum at this conformation; however, this author noted that the potential surface at this point was extremely flat and also experienced similar failures for this conformer at other levels of approximation. In fact, in our MP2 calculations the conformer **5** structure rapidly converts to **1** by a facile rotation of the COOH group, and a similar interconversion with low barrier is possible for conformer **4**; conformers **4** and **5** can therefore be considered to form a metastable sub-group, and **2** and **3** likewise constitute a closely related sub-group in the conformational space of this molecule.

The calculated vertical ionization energies (IEs) for the B3LYP/6-31G** structures **1**−**5** are listed in Table 2 and their positions marked in Figure 2. It has previously been remarked that the ionization energies of **1** show a distinctly better correspondence with the He I PES than do those obtained for

TABLE 2: Calculated (ROVGF/cc-pVDZ) Alanine Ionization Energies (eV)

	conformer[a]					conformer[b]			zwitterion[c]
orbital no.	**1**	**2**	**3**	**4**	**5**	**1**[b]	**2**[b]	**3**[b]	**6**
10	24.56	24.73	24.86	24.47	24.42	24.63	24.79	24.90	26.73
11	22.03	21.84	21.80	22.01	22.13	22.08	21.86	21.83	27.35
12	19.64	19.56	19.54	19.89	19.62	19.62	19.53	19.56	22.12
13	17.30	18.26	17.59	16.98	17.21	17.37	18.23	17.64	20.49
14	17.00	16.87	17.63	16.94	17.03	16.96	17.01	17.63	18.00
15	16.60	15.99	16.42	16.98	16.78	16.67	16.08	16.47	16.58
16	15.37	15.40	15.14	15.27	15.51	15.45	15.35	15.24	15.01
17	14.84	15.04	15.10	14.66	14.76	14.78	15.09	15.07	14.40
18	14.82	14.51	14.36	14.94	14.59	14.90	14.48	14.31	14.18
19	13.59	14.06	13.93	13.39	13.30	13.57	14.07	13.95	13.73
20	13.22	12.86	12.93	13.04	13.04	13.27	12.89	13.00	12.54
21	12.58	13.01	12.96	12.73	12.62	12.62	12.99	13.00	11.77
22	11.88	10.96	11.08	11.38	11.85	11.86	10.99	11.07	8.46
23	10.77	11.16	11.05	11.67	11.42	10.79	11.19	11.05	7.56
24	9.58	9.74	9.72	9.27	9.27	9.51	9.68	9.77	7.61

[a] B3LYP/6-31G** optimized geometries. [b] Alternative MP2/6311++G** optimized geometries. [c] No stationary point—nonoptimized geometry.

2 or **3**,[14] and this comparison can be extended with the present experimental results. First, it can be seen that for the three bands above 18 eV there is little to choose between the calculations for any of the conformers. In fact, all seem to overestimate the experimental IEs by a small amount. We have noted just such behavior in a study of camphor[26] and it seems to be indicative of the increased importance of electron correlation for these deeper lying orbitals and corresponding limitations of the one-particle model for ionization adopted in the OVGF treatment.

Below 18 eV, however, the calculated IEs for conformer **1** again seem considerably better matched to the experiment; there is almost a 1:1 correspondence between observed peak positions and ROVGF calculations for **1**. Those calculated IEs (15.37, 17.0, 17.3 eV) which do not directly correspond to distinct structures in the spectrum may nevertheless correspond to weak but discernible shoulders in the PES. The only significant discrepancy is the lack of a predicted peak matching the experimental peak at 14.3 eV. Here we draw attention to the two nearly identical calculated IEs at 14.8 eV (orbitals 17,18, **1**, Table 2). One may speculate that if either of these ought, for some reason, to be shifted to lower IE there would then be an improvement, reducing this one apparent flaw in the correlation with experiment.

Both conformers **2** and **3** may be deemed to provide a worse match to the experimental spectra. While neither has quite such a problem with the 14.3 eV structure, neither predicts the correct position for the experimentally very distinct third peak at 11.8 eV and **2** even predicts a band in what is a clear valley in the experiments, just above 18 eV. Neither **4** nor **5** provides a good match to the experimental data in the 10−18 eV region. At this point we thus conclude, as before,[14] that a dominant contribution is made by the conformer structure **1**, with possible weaker contributions by **2** and/or **3**. As discussed in the Introduction, other experimental evidence also suggests that the dominant structure encountered in a gaseous sample is **1** with a much smaller contribution from **3**.[9,10] Structures **1**−**3** have the lowest calculated energies (Table 1), and since there is no significant evidence to indicate a role for independent structures **4** or **5** in gaseous samples we will henceforth concentrate our attention on **1**−**3**.

The MP2 calculations (Table 1, ref 7) seem to do a better job, inasmuch as they predict **1** to be the most stable conformer. We have therefore checked that using the geometrical parameters obtained from these MP2 calculations instead of the B3LYP results makes a negligible difference to the calculated IEs, as can be seen from the alternative IE values included in Table 2. We have also taken the opportunity to consider the possible role of a zwitterionic structure, **6**, in these gas-phase experiments. The isolated structure has no stable minimum, either in our calculations or those reported elsewhere,[6] and rapidly converts to **2.** But even when ionization energies are calculated at a presumed structure shown in Figure 1 they deviate so greatly from the experiment (see Table 2) that any involvement of zwitterionic form can be readily dismissed.

4.1.2. Orbital Assignment of Alanine PES Bands. We may now discuss orbital assignments for the alanine PES, assuming the dominant contribution comes from **1**. Of course in a molecule such as this, which lacks elements of symmetry, there is no symmetry-based orbital classification scheme to offer convenient labeling and characterization of the orbitals, which somewhat hampers discussion. We therefore identify the various orbitals (in Table 2 and in the following discussion) principally by just a sequence number, such that they are ordered by ascending eigenvalue. The HOMO is thus orbital 24.

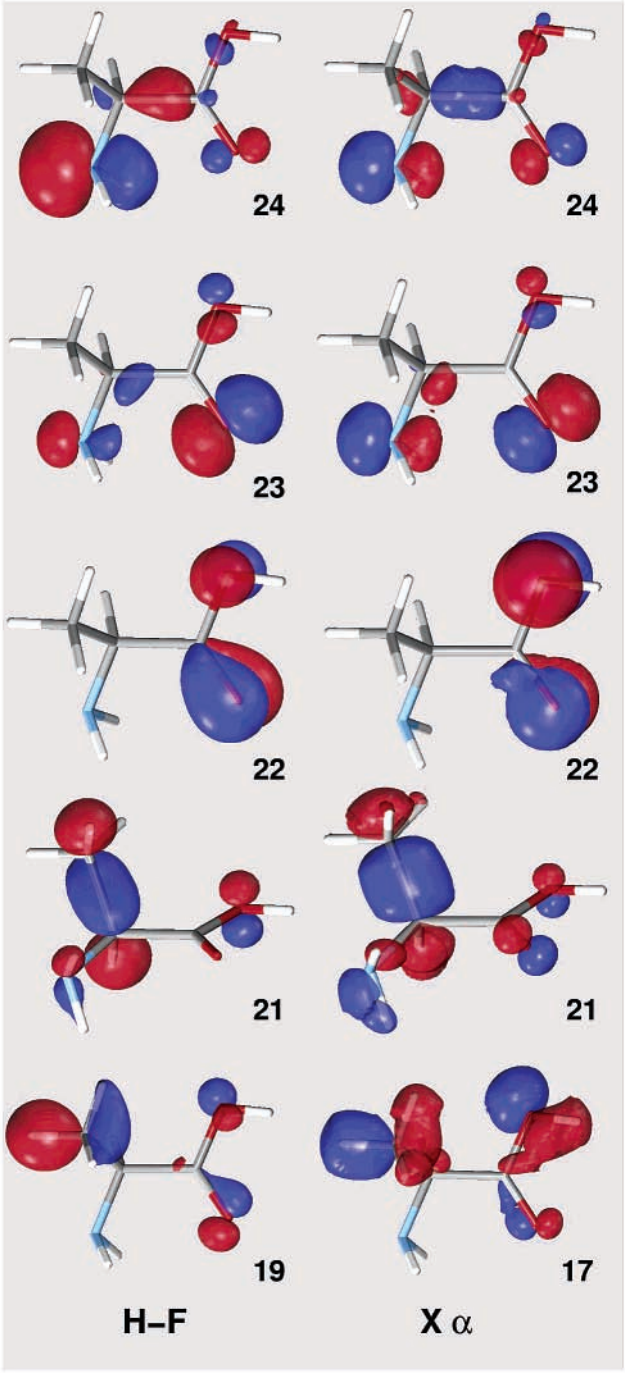

Figure 3. Representative HF/cc-pVDZ orbitals and the corresponding Xα orbitals for structure **1**. The orbital labeling indicates the relative ordering of eigenvalues in each calculation (cf. Table 2 for the HF orbitals).

Some of the computed cc-pVDZ Hartree−Fock orbitals, used for the OVGF calculation for **1**, are shown graphically in Figure 3. From this figure it is seen that the outermost two orbitals, 24 and 23, are primarily a nitrogen and carbonyl oxygen lone pair, respectively, although they are strongly mixed, while the next, 22, is an OCO π^* system. This is in agreement with the assignments for the first three PES bands suggested by Cannington and Ham[13] though earlier workers[11,12] had suggested the third band, orbital 23, be assigned as another O lone pair rather than π orbital.

The next group of three orbitals, 21−19, are dominated by N−H and C−H bonds with 19 being very much a $-CH_3$ orbital yet having some small CO σ characteristic. Of the next three

orbitals, 18 and 17 are best described as skeletal bonding orbitals while 16 is the very characteristic OCO π bonding orbital. Providing a succinct description of the remaining orbitals is quite a challenge!

In comparison to the HeI PES one of the major changes seen at $h\nu = 92$ eV is an enhancement of the relative intensity of the first three peaks. Qualitatively, this may be anticipated to arise from the significant oxygen (and to a lesser extent the nitrogen) atomic 2p character associated with these molecular orbitals.[27] Similarly, one might, empirically, expect the enhancement of the ionization from orbital 16 compared to that from 17, 18 which is observable. Changes in relative band intensities are examined more quantitatively in the next section.

The ordering, and ultimately the characteristics, of the molecular orbitals change when one considers the related conformer pair **2** and **3**. For example, the O and N lone pairs are still strongly mixed but with the relative ordering reversed. And the OCO π^* system shifts to lie between the predominantly n_O HOMO and the interchanged n_N orbitals (see Figure 4). The IEs for the OCO π^* and n_N orbitals then lie very close together in both these conformers.

4.1.3. Simulation of the Alanine PES. We now attempt to simulate not just the peak positions, but their relative intensity and its dependence upon the photon energy in an attempt to shed more light on the participation of the conformers **1**−**3** in the thermal sample. To do this we use the CMS-Xα method to obtain orbital ionization cross-sections. However, the Xα estimation of ionization energies (using Slater's transition state procedure[28]) yields results that are in general (and specifically in this case) much less reliable than those calculated by the OVGF method. To get the closest approach to the experimental spectra we therefore prefer to retain the latter calculations for the positions of the peaks and to associate a CMS-Xα cross-section with each to model the observed peak intensities.

This procedure requires a little care to establish the corresponding orbitals in the two methodologies. Xα is a primitive density functional method. Unlike for the familiar Hartree−Fock orbitals, Koopman's theorem cannot be applied to the Xα orbital eigenvalues (hence the need for the above-mentioned transition state procedure for ionization energies). But there is, therefore, no a priori reason to suppose that the HF and Xα orbitals will have the same relative ordering of eigenvalues and will hence share the same numbering. (Indeed we observe that there can be changes in the relative ordering of the Hartree−Fock orbitals themselves with changing size of the basis set and we take care to consistently use the same cc-pVDZ basis in the following comparisons.) We have therefore carefully examined the HF/cc-pVDZ and Xα orbitals obtained for each of the three conformers in order to establish an exact 1:1 correspondence between the two sets. Some results of this are included in Figures 3 and 4.

The wider issue of the physical interpretation of Kohn−Sham (KS) density functional orbital functions and their use to obtain ionization energies other than the first has been of long-standing interest. Recent work[29−31] has affirmed that for modern functionals and small molecules, at least, there is a correspondence between HF and KS orbitals and between both types and the measured ionization energies. It is perhaps then of some interest to note the similarity observed between these HF and Xα orbitals in a larger molecule once differences in the relative ordering of their eigenvalues are recognized.

The calculated vertical IEs and the corresponding cross-sections can then be presented as a stick spectrum (Figure 5) into which we fold a Gaussian function to give a more realistic

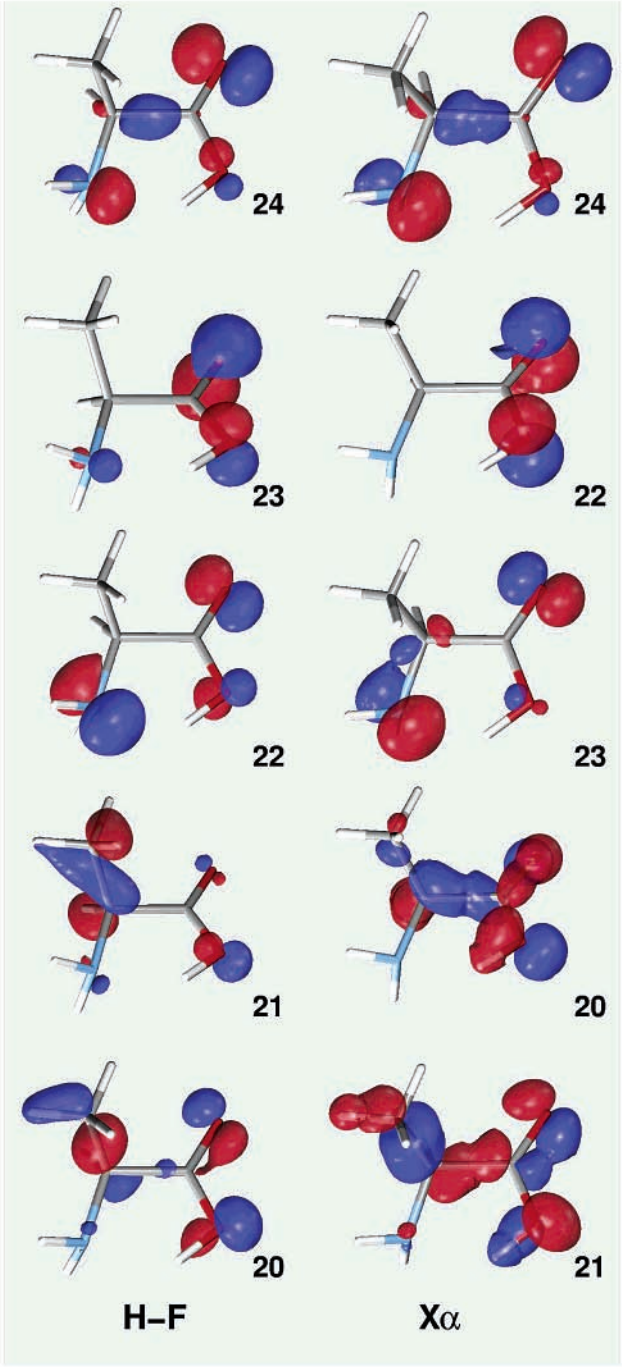

Figure 4. As Figure 3 for the alternative conformer structure **3**.

overall appearance. Examination of the experimental data indicates that perhaps the peak widths increase with increasing IE. This tendency can be rationalized as follows. At low IE, the orbitals are predominantly non- or weakly bonding in character with little vibrational excitation of the ion expected, and hence a relatively narrow Franck−Condon width can be expected for the experimental band; at higher IEs more strongly bonding skeletal electrons are ionized, with greater vibrational excitation. We consequently choose a Gaussian function with width given by the purely empirical formula

$$\Delta E = \left(\frac{\mathrm{IE}}{27 - 0.2 \times \mathrm{IE}}\right)$$

in order to simulate this increase, and maintain the (integrated) peak area proportional to the calculated cross-section.

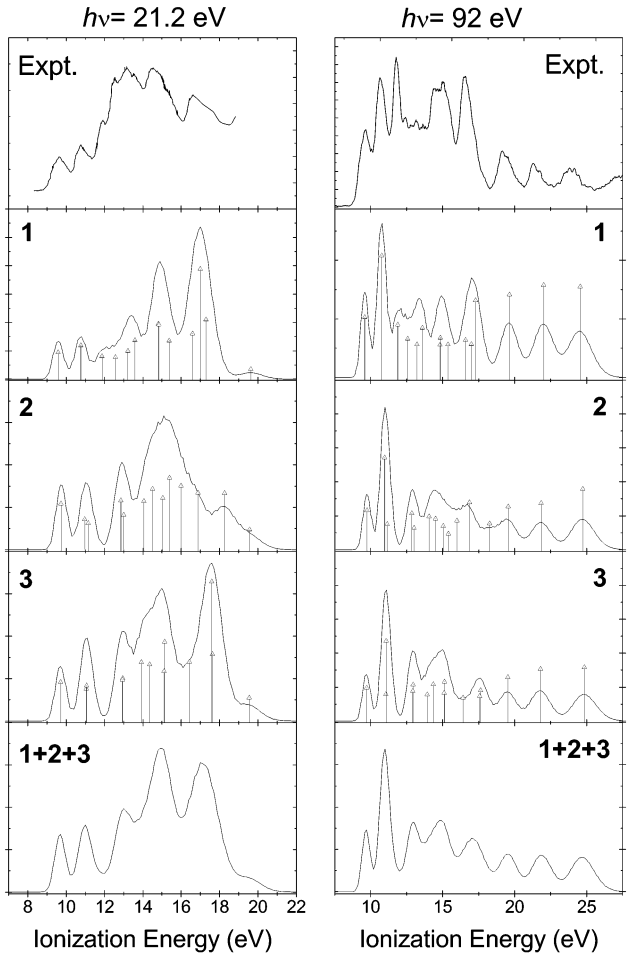

Figure 5. Simulated alanine PES. The calculated positions and cross-sections (vertical bars) are folded with Gaussian functions to achieve a realistic simulation of the final spectra of **1**, **2**, **3**, and their combination. The major tick marks on the *y*-axes are in units of 5 Mb ($h\nu = 21.2$ eV, left column) and 0.2 Mb ($h\nu = 92$ eV, right column). Note the rescaling between the 92 eV plots for **1** and **2**, **3**. Experimental PES from Figure 2 are included at the top of the relevant columns for easy comparison.

From Figure 5 it can be seen that this relatively unbiased choice of Gaussian peak shapes of continuously varying width gives reasonably realistic looking simulated spectra. The simulation for **1** looks particularly close to the experiment and reproduces not just an overall spectral envelope, but more particularly also the changes in relative band intensity at the two different photon energies studied. The profiles of the simulated spectra for **2** and **3** compare less well in a direct comparison with the experimental data.

The predicted relative energies of these three conformers (and hence the expected equilibrium populations) evidently depends on the computational method adopted (Table 1 and ref 7), but the differences are small and almost certainly less than the thermal energy, *kT*, at the ~500 K temperature of the experiments. Consequently, it would be reasonable to assume, without favoring any particular calculation, that there ought to be an essentially equal population of the three conformers. This unbiased assumption would then suggest that an improved simulation ought to result from taking an unweighted addition of the simulations for the three individual conformers. But, in fact, this is *not* found to be the case (Figure 5). Moreover, it is apparent that whatever population/weighting one assumes for **2** and **3** the agreement with experiment is not improved over that displayed by the conformer **1** simulation alone.

4.1.4. Threonine Photoionization. An important experimental task in these investigations is to identify a suitable temperature for the source, affording a reasonable vapor pressure of the sample molecule with consequent acceptable signal intensity. While this proved unproblematic for alanine, significant changes with temperature were noted with threonine, indicating thermal decomposition of the sample. This can be seen in Figure 6. As the temperature reached ~100 °C the main features recorded in the PES were clearly recognizable as those of H_2O (IP 12.62 eV) with a second set of features attributable to CO (IP 14.01 eV) as the temperature rises further toward 200 °C. Nevertheless, there is a clear growth of structure below the water IP at elevated temperatures above 200 °C which may be attributable to threonine, or perhaps some organic decomposition product.

In the only published reference to the threonine PES known to us,[13] its ionization energies are listed as 10.2, 11.05, 11.25, and 12.3 eV. This concurs with the region of the structures we note, but in the absence of a published reproduction of the actual spectrum it is not known how this earlier work may have been affected by decomposition.

To ascertain whether the features are assignable as molecular threonine, we have again calculated the OVGF IE values for this molecule. Four conformations **7**−**10** (see Figure 7) have been considered, each stabilized by the formation of five-membered hydrogen-bonded ring structures. While we have not undertaken an exhaustive search to identify all conformers of this molecule, it is felt that these are a representative subset. The total energies of the B3LYP/6-31G** optimized structures are listed in Table 3, where it is seen that **7** is unambiguously predicted to be the most stable.

A detailed comparison of the experimental 211 °C PES with the IE values calculated for these conformers is presented in Figure 8. The latter are plotted as symbols whose expected contribution, assessed as the predicted 211 °C Boltzmann populations based upon the energies shown in Table 3, is indicated by their height from the abscissa. While this suggests that the higher energy conformers may effectively contribute to a relatively unstructured low-level background in the spectrum below 12.5 eV, the observed peak structures do correspond reasonably closely to the first four IEs (9.74, 10.63, 11.43, and 11.39 eV) calculated for the major conformer, **7**.

4.2. C1s Core Ionization Spectrum of Alanine. An example C1s spectrum of alanine is presented in Figure 9. The most surprising feature is the presence of at least four peaks (the flat-topped nature of the low energy ~291.2 eV peak suggests it may be a partially resolved composite). Our assignment is guided primarily by a previous study of gaseous glycine[32] which reported the following binding energies: $H_2N\underline{\mathbf{C}}H_2COOH$ 292.25 eV; $H_2NCH_2\underline{\mathbf{C}}OOH$ 295.15 eV. This assignment was supported by density functional calculations by Chong[33] which reproduce these binding energies to within 0.2 eV.

In earlier studies of solid zwitterionic amino acids it was also noted that the binding energies at a given functional site were remarkably constant across the range of 20 amino acids.[1] If we assume parallel behavior is obtained in the gas phase, then the 292.3 eV peak in Figure 9 can be assigned as the $\underline{\mathbf{C}}NH_2$ core level and the 295.3 eV peak as the $\underline{\mathbf{C}}OOH$ carboxyl ionization. The core binding shifts in other molecular analogues may be examined to affirm the plausibility of this assignment; for example, the carboxylic C1s binding energy in acetic acid is 295.4 eV, while many methyl C1s binding energies are around 291 eV.[34] We may thus tentatively extend our alanine assignment, identifying the 291.2 eV experimental peak as likely being the $\underline{\mathbf{C}}H_3$ methyl ionization.

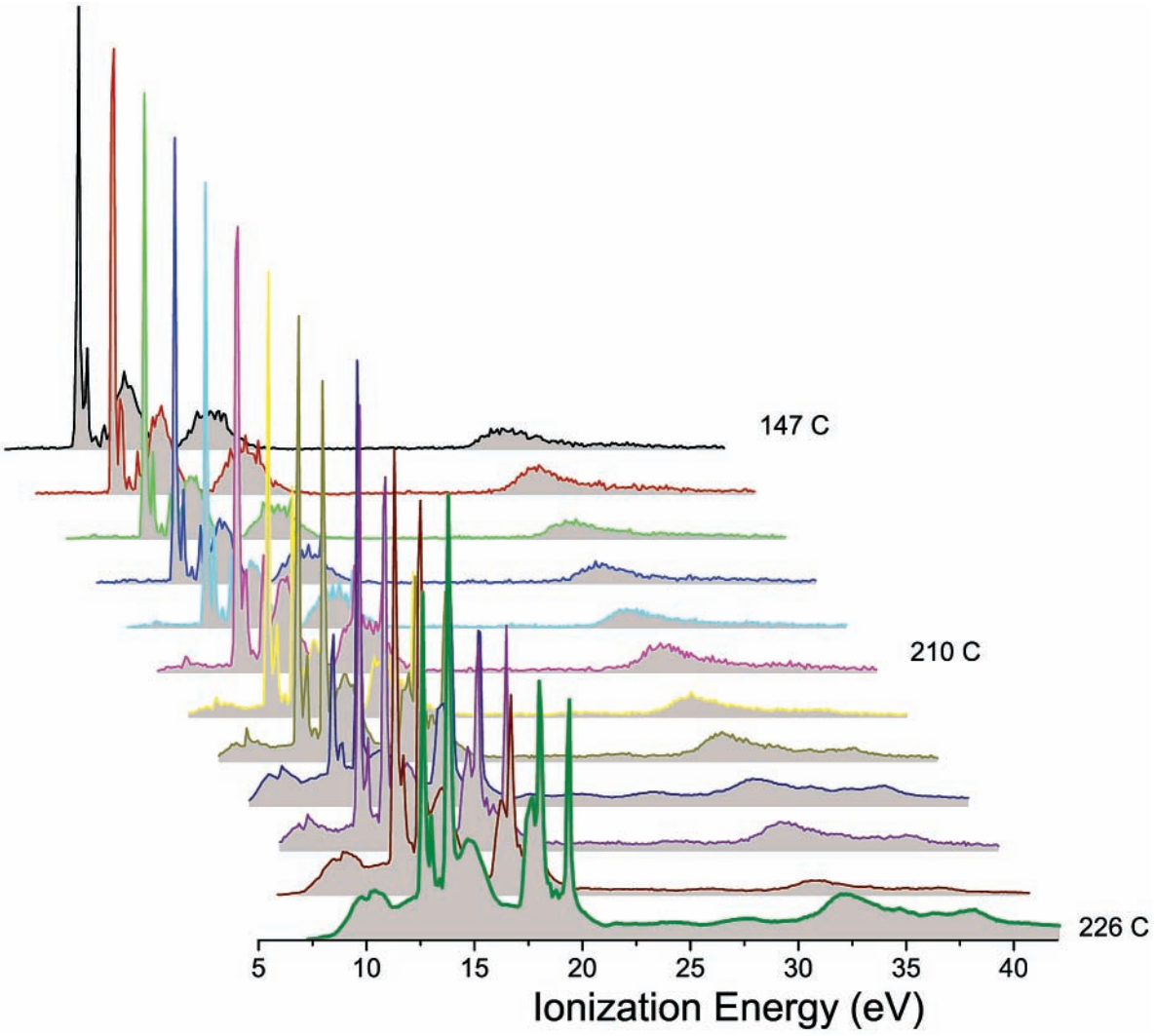

Figure 6. Temperature dependence of the recorded threonine $h\nu = 92$ eV valence photoelectron spectrum.

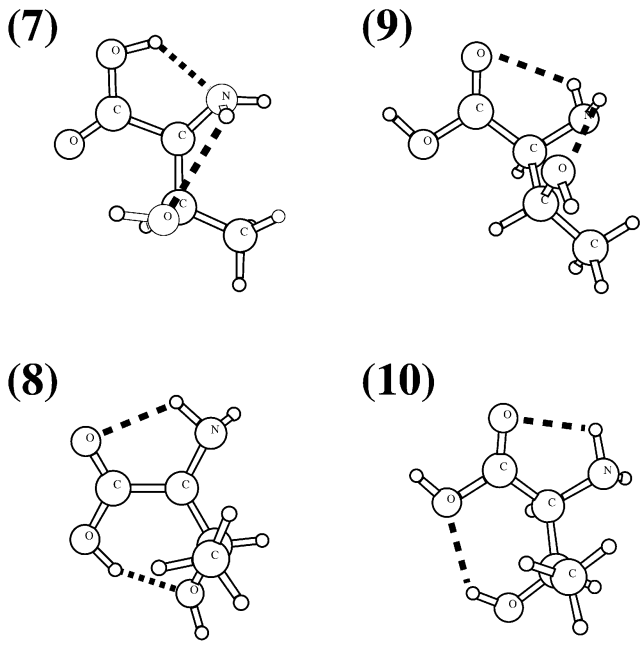

Figure 7. Predicted intramolecularly hydrogen-bonded conformers of threonine.

We support this suggested assignment with a relatively unsophisticated calculation of the Koopman's theorem ionization energies derived from the Hartree−Fock C1s core eigenvalues. These are given in Table 4 for each of the three principal alanine conformers and are plotted in Figure 9, where we have employed a single arbitrary offset of the Koopman's energies in order to bring the theoretical and experimental peak positions into approximate coincidence. In practice, any such estimates based on HF eigenvalues are expected to *overestimate* the binding energy, since relaxation in the core hole state is ignored, which argument may be used to rationalize our offsetting the plot.

TABLE 3: Energies of Optimized Threonine Conformers

	B3LYP/6-31G** energy	
conformer	absolute (a.u.)	relative (cm^{-1})
7	−438.293409	0
8	−438.288796	1012
9	−438.287525	1291
10	−438.286579	1499

Koopman's theorem does not strictly apply to the DFT Kohn−Sham orbitals calculated with present-day functionals such as B3LYP. However, studies suggest that *relative* ionization energies may still be meaningfully estimated from DFT results[30] and that the eigenvalues may be related to the Koopman's theorem limit by a simple linear correlation.[29] More particularly, these studies find that the Kohn−Sham orbitals are generally shifted to higher (less negative) energy than their HF counterparts and are consequently more likely to *underestimate* the binding energy. Overall, the HF and DFT eigenvalues, which

TABLE 4: Koopman's Theorem[a] C1s Core Binding Energies (eV) for Alanine Conformers 1−3

	HF/cc-pVDZ			B3LYP/6-31G**			mean of HF & DFT results		
carbon site	**1**	**2**	**3**	**1**	**2**	**3**	**1**	**2**	**3**
−COOH	280.78	280.40	280.34	309.68	309.42	309.48	295.23	294.91	294.91
$H_2NCHCOOH$	278.43	278.75	278.72	306.89	307.25	307.33	292.66	293.00	293.02
$-CH_3$	277.16	277.34	277.53	305.60	305.81	306.12	291.38	291.57	291.83

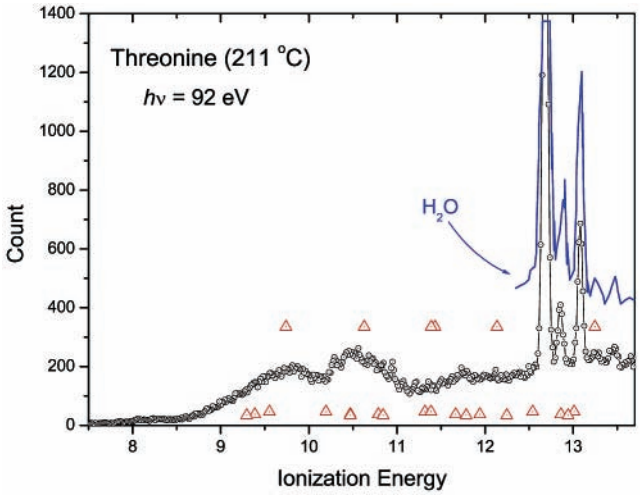

Figure 8. Detail of threonine $h\nu = 92$ eV valence photoelectron spectrum. The symbols indicate calculated vertical IE values for the conformers **7**−**10**, and their height above the axis is proportional to the expected thermal equilibrium population of that conformer. The He I PES of H_2O is overplotted.

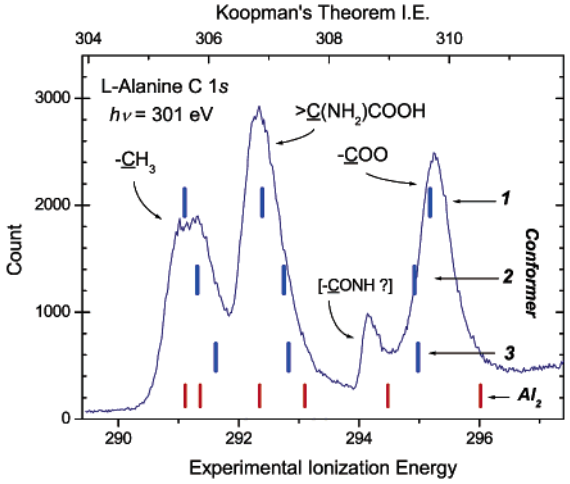

Figure 9. The $h\nu = 301$ eV C1s level core ionization spectrum of alanine. The HF/cc-pVDZ core eigenvalues (Koopman's theorem IEs) are also marked with a scale offset chosen to cause them to coincide with the experimental peaks (see text).

are also given in Table 4, should generate estimates which bracket the experimental ionization energy and both should reliably indicate the expected *relative* shifts.

The final columns in Table 4 present the mean binding energy estimates derived from the HF and DFT treatments. Of course there is no rigorous scientific basis for such a simple averaging, but it serves to emphasize that the experimental values are indeed rather symmetrically bracketed by the two estimates, and that the relative splittings in either case are in close accord with experiment.

It can be seen from Figure 9 that the Koopman's theorem binding energies, particularly those for structure **1**, map closely onto the three major peaks of the spectrum after the correctional offset is applied. Conformation **1** has, of course, already been identified as the dominant gas-phase structure. The data shown in Figure 9 thus corroborate both the assignments suggested for the major peaks and the dominant contribution made by conformer **1**.

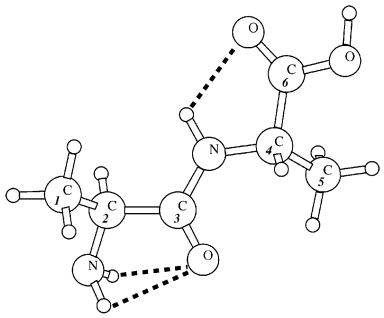

Figure 10. L-Alanyl-L-alanine. B3LYP/6-31G** optimized structure, showing stabilizing hydrogen-bonded five-membered ring formation.

It remains to identify the smallest 294.15 eV peak which is a fairly reproducible feature seen in spectra recorded at differing photon energies. It seems unlikely to be a thermal decomposition product. Unlike threonine, where such products are clearly visible in the valence PES, there is no indication of decomposition in the same source and at the same temperature in the valence spectrum of alanine itself. Moreover, no indication of potential decomposition products such as CO (BE 296.2 eV) or CO_2 (BE 297.7 eV) was found in either of these regions and further browsing through Jolly's compilation of core binding energies[34] fails to reveal any plausible organic decomposition products, or sample contaminants, having peaks in the vicinity of 294 eV.

However, we speculate that the minor 294.15 eV peak might possibly result from a polymerization rather than thermal decomposition, and that this may, in some way, be initiated by soft X-rays (hence not seen in the VUV experiments). Certainly, in studies of the solid amino acid lysine at the same photon energies Bozack et al.[35] detected structural changes after exposure which were deduced to be photolytically induced (rather than related to some substrate heating effect). The enclosed nature of the source cell employed in the current experiments may, however, also facilitate such a process due to the proximity of heated surfaces or simply by helping retain any such products in the source region.

The most likely outcome of a polymerization would be formation of a peptide linkage, CONH. Chong et al.[36] have recently published calculations of the core binding energies for two model dipeptides which return values $\sim 293.9 \pm 0.15$ eV for the carbonyl carbon in the peptide bond. This is the closest match found for the minor peak in the alanine spectrum. To explore this hypothesis more specifically we have then extended our Koopman's theorem calculations to treat the simplest possibility, formation of the dipeptide alanylalanine from two alanine monomers.

Figure 10 shows the lowest energy alanylalanine conformation we located with B3LYP/6-31G** geometry optimization. A very recent paper[37] has undertaken the same calculation as part of a more extensive study of small dipeptide molecules, identifying the same conformation as that here. C1s eigenvalues have then

TABLE 5: Koopman's Theorem[a] C1s Core Binding Energies (eV) for L-Alanyl-L-alanine

atom[b]	description	HF/cc-pVDZ	B3LYP/6-31G**	mean of HF and DFT results
C1	$\underline{C}H_3$	305.61	276.97	291.29
C2	$\underline{C}$(NH2)(Me)(CO−)	306.85	278.16	292.50
C3	$\underline{C}$O−NH	308.98	279.77	294.37
C4	$\underline{C}$(NH−)(Me)(COOH)	307.60	278.95	293.27
C5	$\underline{C}H_3$	305.86	277.31	291.58
C6	$\underline{C}$OOH	310.52	281.39	295.96

[a] i.e., the negated orbital eigenvalues. [b] See Figure 10.

been calculated following the same procedures as for alanine and the results presented in Table 5. These are not expected to be highly sensitive to any changes in the conformation of the dipeptide.

The HF Koopman's theorem estimates from Table 5 are marked on the spectrum in Figure 9, using the same offset scale as was used for marking up the analogous alanine binding energy estimates. This means that in making a visual comparison of the predictions and the experimental peak positions using this figure we are effectively assuming the same correction for the neglected core relaxation energy as was empirically adopted for alanine. While this may be an imperfect assumption it can be seen that, as anticipated from the much more sophisticated calculation by Chong et al.,[36] the estimated peptide C1s peak position maps closely to the minor experimental peak, while the other C1s binding energies obtained for this dipeptide could conceivably be substantially obscured beneath the major peaks previously assigned to alanine. In fact, it requires only a small additional offset to the estimated energies to make this suggestion look very convincing.

5. Conclusions

Using ab initio calculations of the vertical ionization energies and adding information obtained from CMS-Xα calculations of the orbital ionization cross-sections it is possible to account well not just for the features of a new $h\nu = 92$ eV photoelectron spectrum of gaseous alanine, but also the differences seen in earlier $h\nu = 21.2$ eV spectra, considering just a single possible conformer, that labeled **1**. Even the much simpler analysis offered for the C1s core level spectrum looks most convincing for **1**. Photoelectron spectroscopy does not offer a definitive identification of the conformations present, but especially in the valence region it is quite evident that no real improvements to the simulated spectra result from considering even partial contributions made by other candidate structures, **2** or **3**, and unambiguously **1** is the dominant structure. This contrasts with an analogous study performed with butan-2-ol where evidence for the contributions made by alternative molecular conformations present in the thermal sample could be clearly identified.[38]

The conclusion arrived at in the present case corroborates other experimental gas-phase studies of alanine[5,8−10] which have **1** in at least an 8-fold excess. This greatly exceeds the range of thermal population differences based upon various calculations of the relative conformational energies. This conundrum has already been considered at length[5,10] to which discussion we can add that the present deduction is based on experiments using not a molecular beam but a heated gas cell; a true thermal equilibrium can be assumed. Thus the anomaly does not rest upon nonequilibrium relaxation effects that may arise in a beam source.

The B3LYP/6-31G** calculations and the previous MP2/6-311++G** calculations[7] repeated here both indicate that the conformers **1**−**3** are very close in energy, so much so that it is no surprise that the predicted energetic ordering, based upon such extremely small differences, should be method-dependent. What *is* significant is the clear inference from either that essentially equal thermal populations would be expected. It remains to be seen whether even higher level calculations would revise this prediction, which is otherwise seen to be at odds with the experimental findings of a dominant conformation **1**.

The experiments on another amino acid, threonine, are limited by the very evident decomposition, producing at least H_2O and CO at the elevated temperatures required to produce a sufficient sample vapor pressure. Nevertheless, broad features seen below 12 eV would appear to be attributable to molecular threonine as they correspond reasonably well to the vertical ionization energies predicted by calculation for this species. Even the rather low definition may be in part due to an underlying contribution from many less stable conformers in the equilibrium sample.

The experience with threonine does, however, provide some confidence that alanine is not so afflicted by thermally induced decomposition, for none of the very clear evidence in the threonine PES is seen with alanine. This is important in the analysis of the C1s alanine spectrum. The three major peaks are fairly readily assigned to the three carbons in the alanine molecule—most likely, as mentioned above, in conformation **1**. A fourth minor peak is somewhat more difficult to explain. There is no internal evidence in either the valence or core spectra for the production of CO_n which might accompany thermal dissociation, nor have we been able to identify any such organic products which might give rise to the minor peak. However, speculation that alanine may be polymerizing via the formation of peptide linkages can be supported by calculations that make the assignment of the minor peak to $\underline{C}$ONH plausible.

Though a priori unexpected there may be arguments to explain such condensation stemming from the use here of a heated gas sample cell. First it provides heated (maybe catalytic) surfaces in proximity to the ionization volume. Second, the pressure in the cell is intentionally elevated, probably by at least 2 orders of magnitude over that we measure in the main chamber. Third, the continuous irradiation by energetic soft X-rays may itself induce sample reaction. Finally, any products that are created will be partially trapped in the cell and may tend to accumulate with time (though we noticed no temporal variation in this peak's intensity). In the future, repeated experiments made with a molecular beam source, continuously swept from the ionization region, may help shed further light on this matter.

Assuming, however, that the dipeptide hypothesis has some substance, it is necessary to consider whether it could play a role in the valence spectrum. Identical experimental conditions pertained, except for the use of a lower energy photon beam. Thus three of the four preceding arguments remain as valid. The principal deficiency noted between the experiment and the best simulations was in the region 14−15 eV where the experimental peak structure was not well reproduced theoretically. This has been examined by calculating ionization energies in just the same fashion as for the other species detailed here.

The greater size of alanylalanine means that there is an increased density of ionic states in the 9−18 eV region. Hence, while the calculation does suggest a peak at 14.46 eV, this is just one of many which are found distributed pseudo-uniformly over the range. In other words, the overall correlation of predicted features with experiment is poor. So while a definitive answer cannot be reached, there is no compelling reason to invoke a contribution from this or from any other species considered other than alanine conformer **1**.

This then drives one back to examine differences between the VUV and X-ray experiments and to the consideration that effects of the more energetic photon beam may be the key factor. Photon-induced "damage" to solid samples caused by intense synchrotron X-ray beams is of course a recognized phenomenon and has been previously reported to affect amino acid samples;[35] perhaps in the conditions of our experiment the energy deposited by the beam is resulting in creation of reactive ion and radical fragments which could be polymerizing on recombination.

Notwithstanding these questions, the present work has succeeded in proving the ability to interpret gas-phase electron spectra of biologically important molecules using electronic structure calculations.

Acknowledgment. We thank the staff at BESSY for assistance in operating the beamline. Computational resources on a COMPAQ ES40 multiprocessor cluster (Columbus) at the Rutherford Appleton Laboratory (RAL) were provided by the U.K. Computational Chemistry Facility. We gratefully acknowledge partial support by the Deutsche Forschungsgemeinschaft. and by INTAS Grant 97-471.

References and Notes

(1) Clark, D. T.; Peeling, J.; Colling, L. *Biochim. Biophys. Acta* **1976**, *453* (2), 533−545.

(2) Nyberg, M.; Hasselstrom, J.; Karis, O.; Wassdahl, N.; Weinelt, M.; Nilsson, A.; Pettersson, L. G. M. *J. Chem. Phys.* **2000**, *112* (12), 5420−5427.

(3) Williams, J.; Haq, S.; Raval, R. *Surf. Sci.* **1996**, *368*, 303−309.

(4) Cao, M.; Newton, S. Q.; Pranata, J.; Schafer, L. *Theochem. J. Mol. Struct.* **1995**, *332* (3), 251−267.

(5) Godfrey, P. D.; Brown, R. D.; Rodgers, F. M. *J. Mol. Struct.* **1996**, *376*, 65−81.

(6) Kaschner, R.; Hohl, D. *J. Phys. Chem. A* **1998**, *102* (26), 5111−5116.

(7) Csaszar, A. G. *J. Phys. Chem.* **1996**, *100* (9), 3541−3551.

(8) Iijima, K.; Beagley, B. *J. Mol. Struct.* **1991**, *248* (1−2), 133−142.

(9) Godfrey, P. D.; Firth, S.; Hatherley, L. D.; Brown, R. D.; Pierlot, A. P. *J. Am. Chem. Soc.* **1993**, *115* (21), 9687−9691.

(10) Iijima, K.; Nakano, M. *J. Mol. Struct.* **1999**, *486*, 255−260.

(11) Debies, T. P.; Rabalais, J. W. *J. Elec. Spectrosc. Relat. Phenom.* **1974**, *3*, 315−322.

(12) Klasinc, L. *J. Elec. Spec. Relat. Phenom.* **1976**, *8*, 161−164.

(13) Cannington, P. H.; Ham, N. S. *J. Elec. Spectrosc. Relat. Phenom.* **1983**, *32* (2), 139−151.

(14) Powis, I. *J. Phys. Chem. A* **2000**, *104* (5), 878−882.

(15) Weiss, M. R.; Follath, R.; Sawhney, K. J. S.; Senf, F.; Bahrdt, J.; Frentrup, W.; Gaupp, A.; Sasaki, S.; Scheer, M.; Mertins, H. C.; Abramsohn, D.; Schäfers, F.; Kuch, W.; Mahler, W. *Nucl. Instrum. Methods Phys. Res. A* **2001**, *467* (1), 449−452.

(16) Mårtensson, N.; Baltzer, P.; Brühwiler, P. A.; Forsell, J.-O.; Nilsson, A.; Stenborg, A.; Wannberg, B. *J. Elec. Spec. Relat. Phenom.* **1994**, *70* (2), 117−128.

(17) Seah, M. P. *Surf. Interface Anal.* **1993**, *20* (3), 243−266.

(18) Becke, A. D. *J. Chem. Phys.* **1993**, *98* (7), 5648−5652.

(19) Lee, C. T.; Yang, W. T.; Parr, R. G. *Phys. Rev. B* **1988**, *37* (2), 785−789.

(20) Frisch, M. J.; Trucks, G. W.; Schlegel, H. B.; Scuseria, G. E.; Robb, M. A.; Cheeseman, J. R.; Zakrzewski, V. G.; Montgomery, J. A.; Stratmann, R. E.; Burant, J. C.; Dapprich, S.; Millam, J. M.; Daniels, A. D.; Kudin, K. N.; Strain, M. C.; Farkas, O.; Tomasi, J.; Barone, V.; Cossi, M.; Cammi, R.; Mennucci, B.; Pomelli, C.; Adamo, C.; Clifford, S.; Ochterski, J.; Petersson, G. A.; Ayala, P. Y.; Cui, Q.; Morokuma, K.; Malick, D. K.; Rabuck, A. D.; Raghavachari, K.; Foresman, J. B.; Cioslowski, J.; Ortiz, J. V.; Baboul, A. G.; Stefanov, B. B.; Liu, G.; Liashenko, A.; Piskorz, P.; Komaromi, I.; Gomperts, R.; Martin, R. L.; Fox, D. J.; Keith, T.; Al-Laham, M. A.; Peng, C. Y.; Nanayakkara, A.; Challacombe, M.; Gill, P. M. W.; Johnson, B. G.; Chen, W.; Wong, M. W.; Andres, J. L.; Gonzalez, C.; Head-Gordon, M.; Replogle, E. S.; Pople, J. A. *Gaussian 98*, Revision A.9; Gaussian Inc., Pittsburgh, PA, 1998.

(21) von Niessen, W.; Schirmer, J.; Cederbaum, L. S. *Comput. Phys. Rep.* **1984**, *1* (2), 57−125.

(22) Zakrzewski, V. G.; Dolgounitcheva, O.; Ortiz, J. V. *J. Chem. Phys.* **1996**, *105* (19), 8748−8753.

(23) Dill, D.; Dehmer, J. L. *J. Chem. Phys.* **1974**, *61*, 692−699.

(24) Davenport, J. W. *Phys. Rev. Lett.* **1976**, *36*, 945−948.

(25) Powis, I. *J. Chem. Phys.* **1997**, *106*, 5013−5027.

(26) Rennie, E. E.; Powis, I.; Hergenhahn, U.; Kugeler, O.; Garcia, G. A.; Lischke, T.; Marburger, S. *J. Elec. Spectrosc. Relat. Phenom.* **2002**, *125*, 197−203.

(27) Schweig, A.; Thiel, W. *Mol. Phys.* **1974**, *27*, 265.

(28) Slater, J. C. *Quantum theory of molecules and solids*; The self-consistent field for molecules and solids; Mc-Graw Hill: New York, 1974; Vol. 4.

(29) Stowasser, R.; Hoffmann, R. *J. Am. Chem. Soc.* **1999**, *121*, 1 (14), 3414−3420.

(30) Politzer, P.; Abu-Awwad, F.; Murray, J. S. *Int. J. Quantum. Chem.* **1998**, *69* (4), 607−613.

(31) Politzer, P.; Abu-Awwad, F. *Theor. Chem. Acc.* **1998**, *99* (2), 83−87.

(32) Slaughter, A. R.; Banna, M. S. *J. Phys. Chem.* **1988**, *92*, 2 (8), 2165−2167.

(33) Chong, D. P. *Can. J. Chem.* **1996**, *74* (6), 1005−1007.

(34) Jolly, W. L.; Bomben, K. D.; Eyermann, C. J. *At. Data Nucl. Data Tables* **1984**, *31* (3), 433−493.

(35) Bozack, M. J.; Zhou, Y.; Worley, S. D. *J. Chem. Phys.* **1994**, *100* (11), 8392−8398.

(36) Chong, D. P.; Aplincourt, P.; Bureau, C. *J. Phys. Chem. A* **2002**, *106* (2), 356−362.

(37) Chaudhuri, P.; Canuto, S. *Theochem. J. Mol. Struct.* **2002**, *577* (2−3), 267−279.

(38) Rennie, E. E.; Powis, I.; Hergenhahn, U.; Kugeler, O.; Watson, T. M.; Marburger, S. *J. Phys. Chem. A* **2002**, *106*, 12221−12228.